ELSEVIER

Journal of Nuclear Materials 307–311 (2002) 1430–1435

journal of nuclear materials

www.elsevier.com/locate/jnucmat

Deuterium transport in SiC_f/SiC composites ☆

G.A. Esteban [a,*], A. Perujo [b], F. Legarda [a], L.A. Sedano [c], B. Riccardi [d]

[a] *UPV – EHU, Department of Nuclear Engineering and Fluid Mechanics/E.T.S.I.I.T., 48013 Bilbao, Spain*
[b] *Joint Research Centre – Ispra Site, Environment Institute, 21020 Ispra (VA), Italy*
[c] *CIEMAT, Dpt. Impacto Ambiental de la Energía, 28040 Madrid, Spain*
[d] *ENEA CR Frascati, 00044 Frascati (Rome), Italy*

Abstract

A time-dependent gas-phase isovolumetric desorption technique has been used over a temperature range of 675–1029 K and driving pressures ranging from 13 to 101 kPa, to obtain the deuterium transport parameters diffusivity, D, and solubility, S, in a 3-D SiC_f/SiC composite. The values obtained are: $D(m^2s^{-1}) = 1.1 \times 10^{-4}\ \exp[-107.7\ (kJ/mol)/RT]$, $S(mol\,m^{-3}) = 1.9 \times 10^3\ \exp[-30.2(kJ/mol)/RT]$. The set of measurements performed at the same temperature, 871 K, and different loading pressures 13, 33, 60, 101 kPa, has evidenced a power relationship of solubility versus loading pressure with exponent 0.22, departing from Sieverts' law. These results are compared with the parameters previously obtained for different types of monolithic SiC, and explained on the basis of the physico-chemical phenomena foreseen within its particular structure. The same experiment has been performed with two sets of specimens manufactured using different variants of the hybrid CVI/PIP technique; a negligible variation of transport parameters has been accounted between both groups of specimens.

1. Introduction

Silicon carbide (SiC) has been identified as a suitable material in diverse applications in the blanket of fusion reactors [1–3]. The physical structure of a SiC/SiC_f ceramic matrix composite (CMC) overcomes the brittle behaviour associated to monolithic SiC, showing favourable mechanical properties for structural fusion components [4] of different breeding blanket concepts (TAURO [5,6] (France), DREAM [7] (Japan) ARIES [8] (US), (A-DC) [9]).

The H transport parameters in SiC_f/SiC composites are the factors governing the tritium (H_T) and deuterium (H_D) inventories, permeation and recycling from the components using this type of material. Thus, a precise characterisation of the interaction between hydrogen (H) isotopes and SiC_f/SiC composite is needed when quantifying issues of safety, breeding feasibility, fuel economy and plasma stability for a future fusion reactor using this material.

In the present work a series of gas/phase isovolumetric desorption experiments (IDE), have been undertaken with a SiC_f/SiC composite over a broad range of temperatures, from 675 to 1029 K, and partial pressures ranging from 1.3×10^4 to 10^5 Pa, in order to obtain the H_D transport parameters diffusivity D (m^2s^{-1}) and solubility S ($mol\,m^{-3}$). This is the first measurement performed with any hydrogen (H) isotope wherein H transport parameters are reported for a SiC_f/SiC composite. The transport parameters corresponding to different types of monolithic SiC are reviewed and compared with the composite, the differences being highlighted and explained.

2. Review of existing data

The H isotopes transport parameters in SiC (diffusivity D and Sieverts' constant K_s) reported up to now

☆ Work performed while at Joint Research Centre – Ispra Site, Environment Institute, 21020 Ispra (VA), Italy

* Corresponding author. Tel.: +34-94 601 4272; fax: +34-94 601 4159.
E-mail address: inpesalg@bi.ehu.es (G.A. Esteban).

0022-3115/02/$ - see front matter
PII: S0022-3115(02)01282-5

Table 1
Experimental Sieverts' constants and diffusivities of hydrogen in SiC

Material	K_{s0} (mol m^{-3} Pa$^{-1/2}$)	E_s (kJ mol^{-1})	D_0 (m^{2}s^{-1})	E_d (kJ mol^{-1})	T (K)	Ref.
α-SiC single-crystal			1.09×10^{-6}	229.5	773–1573	[1]
β-SiC single-crystal			2.80×10^{-3}	271.7	773–1573	[1]
Al doped α-SiC			4.04×10^{-8}	142.1	773–1573	[1]
Vapour deposited β-SiC	1.14×10^{-6}	−154.7	1.58×10^{-4}	307.6	1273–1673	[1]
Hot pressed α-SiC			9.04×10^{-5}	201.5	773–1573	[1]
Sintered β-SiC			8.54×10^{-4}	268.4	773–1573	[1]
Vapour deposited β-SiC	2.14×10^{-5}	−58.8	9.80×10^{-8}	182.4	1273–1873	[10]
Sintered SiC	1.30×10^{-3}	0			923–1173	[2]
KT-SiC	6.78×10^{-4}	−35.1	1.08×10^{9}	590.1	1473–1673	[3]

are shown in Table 1. The results show some deviation from one another. The most probable reasons may be the following:

- the different allotropic structures measured in each case (α-hexagonal or β-cubic); the presence of different levels of doping agents (e.g. Al_2O_3 used as a binder additive for hot sintering) and other impurities;
- excess in C or Si from the stochiometric composition;
- the various types of manufacturing procedure used (powder sintering, hot compression, chemically vapour deposition)
- the particular conditions carried out in each case, these variable production techniques lead to diverse SiC microstructures (single-crystal, polycrystalline structure), different grain size and different content of the amorphous phase.

Causey et al. [1] measured the H_T diffusivities and H_D solubilities in different types of silicon carbide (α-SiC single-crystal, β-SiC single-crystal, Al doped α-SiC single-crystal, vapour deposited β-SiC, hot pressed α-SiC and sintered β-SiC). They performed independently diffusion and solubility measurements; the H_T diffusivity was evaluated for each type of SiC by measuring the release transients of gaseous tritium during isothermal anneals (773–1573 K) of samples recoil injected with tritons. The H_D solubility was separately evaluated in vapour deposited β-SiC by gas evolution loading/deloading measurements; a pressure dependence of solubility close to 0.5 was verified accounting for atomic solution (Sieverts' law). Katsuta and Katano [2] performed a gas evolution method composed by two independent phases (loading and anneal deloading) to measure the hydrogen solubility in hot-pressed SiC. The temperature range investigated was 923–1173 K and pressures from 2.7×10^4 to 10^5 Pa. They accounted for Sieverts' law fulfillment but, simultaneously, certain H inventory adsorbed on the surface of the sample was detected. The main drawback for this experiment is that full saturation of the SiC specimen (dimensions: 10 mm × 10 mm × 1 mm) has been considered in 7 h of loading through the whole experimental temperature range. Verghese et al. [3] measured the protium (H_P) diffusivity and solubility in KT-SiC (manufactured by wet extrusion and sintering) in the temperature range 1473–1723 K and pressures from 2×10^3 to 5×10^4 Pa. The diffusivity values were measured by modelling gas permeation transients, whereas the solubility values were evaluated by annealing the specimen after a loading period. The high diffusivities reported were explained in terms of accelerated diffusion through pores or other microstructural defects. The square root dependence on pressure of the solubility was assumed without explicitly analyzing the available data. Causey et al. [10] measured the H isotopes (99% H_D, 1% H_T) solution and migration but in vapour deposited β-SiC by means of a gas evolution study in the temperature range 1273–1873 K and pressures from 10^3 to 10^5 Pa. A deviation of the solubility dependence on the square root of the loading pressure (Sieverts' law) was explained by the presence of the H_T inventory adsorbed on the surface of the specimen.

3. Experimental

The material studied is a SiC_f/SiC composite [11]. Two sets of specimens supplied by ENEA, showing similar porosity (20%) and volumetric fraction of fibre content (30%), were investigated. Each group consisted of three cylinders with a 6-mm diameter and 60-mm height. The specimen dimensions were defined in this manner to make feasible the H transport study using the approximation to infinite-cylinder geometry. Each set of specimens were manufactured by combining the chemical vapour infiltration (CVI) technique with the polymer infiltration and pyrolysis (PIP) technique and applying different filling times for CVI and the same number of cycles (7) for PIP. The SiC fibre woven fabric preform is composed by Nicalon CG fibres, which is overcoated by a carbon interphase before matrix densification. A

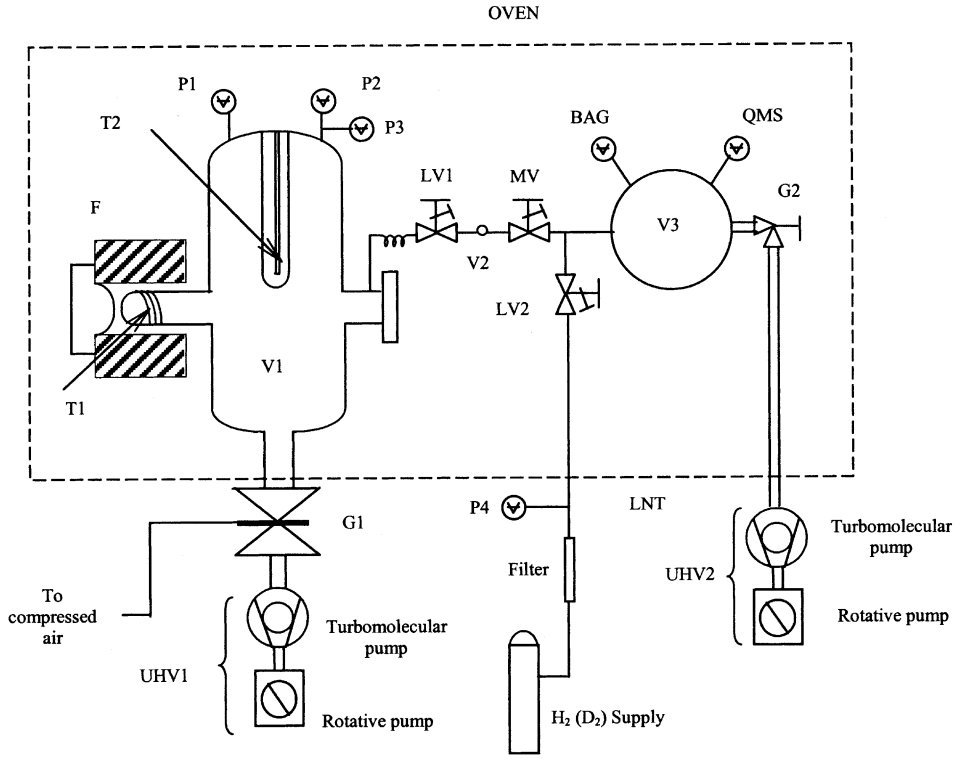

Fig. 1. Schematic view of the isovolumetric desorption facility. BAG – Bayard–Alpert Gauge, MV – manual magnetic valve, F – furnace, P1, P2, P4 – capacitance manometers, P3 – spinning rotor gauge, G1– Electropneumatic gate valve, UHV – ultrahigh vacuum pumping units, QMS – Quadrupole mass spectrometer, G2 – manual gate valve, V1 – experimental chamber, T1, T2: Pt resistance thermometers, V2, V3 – expansion volumes, LV1,2 – manual leak valves.

detailed description of the material has been provided elsewhere [11].

The specimens were investigated as received. Before the set of experiments with gas, a thorough pump down at high temperature (1029 K) was performed to obtain a good vacuum level (10^{-7} Pa).

A schematic view of the experimental installation is shown in Fig. 1. This installation and the procedure for a measurement have been described in detail elsewhere [12]. Briefly, a single run consists of recording, for the release period τ_r, the pressure increase in the constant volume vessel V1 due to the isothermal outgassing from the specimens, which have been previously loaded with H at a given pressure and temperature during a certain period of time τ_1. A short ($\simeq$30 s) but thorough pumping-down period (τ_p) separates the two previous phases (loading and release) in order to evacuate the experimental chamber before the subsequent release phase.

4. Modelling

The slow H migration kinetics in saturation of the samples entails months, even years, in the loading and release processes. Because this action would be too long with the subsequent stability problems in the measuring devices, IDE is performed under non-saturation condition. This non-saturation condition requires the use of a non-stationary model to reproduce the H pressure rise during the release phase [13–16]. The release rate model solves the radial diffusion equation (second Fick's law) in an infinite long cylinder geometry linking all the three phases (loading, pumping and release) and provides transient gas concentration profiles for each single phase. The effective transport parameters D and S are evaluated for each experimental temperature using a non-linear least-squares fitting of the theoretical H pressure increase to the pressure increase measured in the experimental chamber (Fig. 2). The theoretical expression for the measured pressure is [14]:

$$p(t) = \frac{RT}{(V - 3V_s)} 4\pi h \sum_{n=1}^{\infty} \frac{1}{\alpha_n^2} [1 - \exp(-D\alpha_n^2 t)] \times [S(1 - \exp(-D\alpha_n^2 \tau_1)) \exp(-D\alpha_n^2 \tau_p) - c_f] \quad (1)$$

where V_s is the volume of one of the three identical specimens measured simultaneously, V the volume of the experimental chamber, h the height of the specimens.

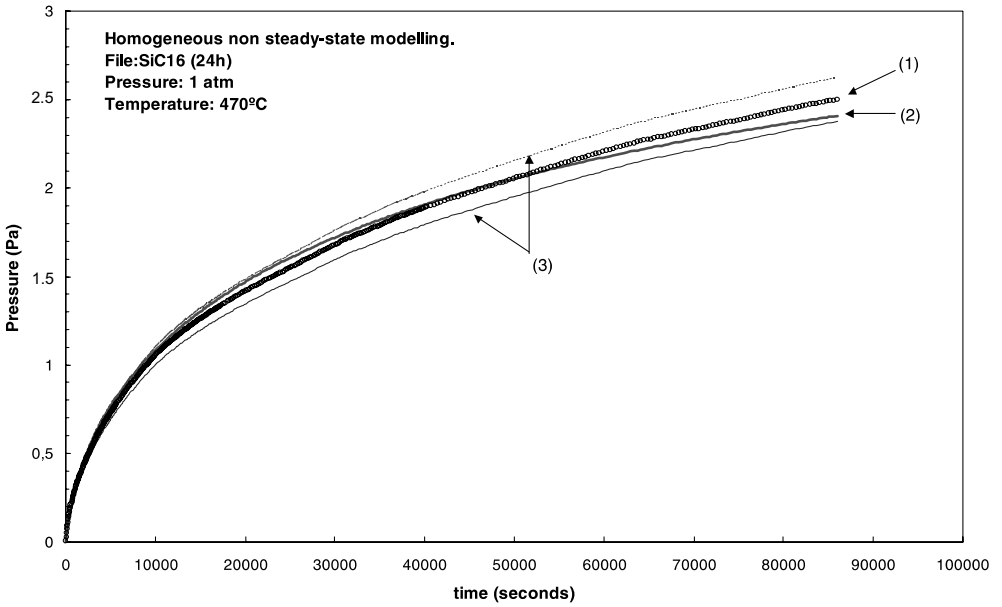

Fig. 2. Experimental release curve fitting. (1) Experimental, (2) Fitting and (3) ±5% pressure margins.

α_n $(n = 1, 2, \ldots)$ are the infinite real roots of the equation $J_0(a\alpha_n) = 0$, a is the cylinder radius and c_f (mol m^{-3}) is the H concentration at the subsurface of the cylindrical specimens at the end of the release phase and S (mol m^{-3}) the solubility at the loading pressure.

Once the transport parameters have been obtained at each temperature, another fitting routine is run with the Arrhenius expressions $S = S_0 \exp(-E_s/RT)$, $D = D_0 \exp(-E_d/RT)$, obtaining the diffusivity D_0 and solubility S_0 preexponentials and the activation energies of diffusion E_d and solution E_s.

5. Results and discussion

A set of four measurements at the same temperature, 871 K, at different pressures 13, 33, 60, 101 kPa, have been performed to check for a possible influence of surface effects on the measurements [17]. The normalised pressure release curves have overlapped each other within the experimental accuracy of the manometers, indicating equivalent transport kinetics for different loading pressures; this fact is evidence for negligible surface effects.

As a consequence, the surface reactions of adsorption and desorption may be supposed to occur infinitely faster compared to the bulk ones. Thus, the deuterium inventory adsorbed on the connected porosity during the loading phase is completely desorbed during the pump-down period.

The variation of the solubility with the loading pressure is shown in Fig. 3. Sieverts' law, $S = K_s p^{1/2}$ (K_s being Sieverts' constant, p the loading pressure, S the solubility), is not fulfilled (exponent 0.22 ± 0.03); this power reduction has been previously reported (exponent 0.37) for SiC in [10]. From these results, it can be assumed that H_D dissolves atomically in the composite (the exponent deviates from 0.5 but even more from the value 1 that describes the molecular absorption). Sieverts' law is not fulfilled probably because of irreversible trapping in defects of the matrix such as internal

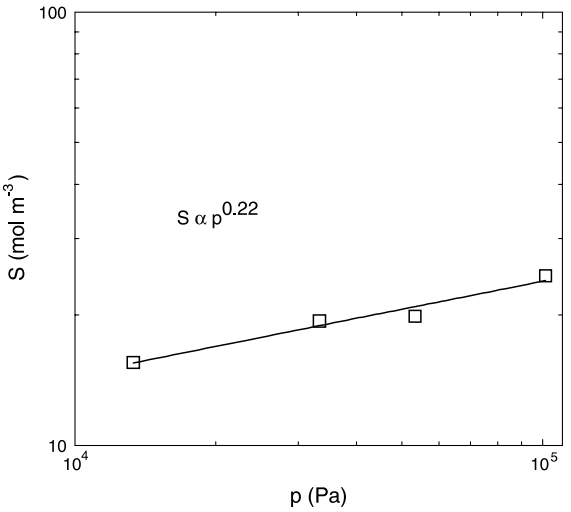

Fig. 3. Solubility for different pressures at the same temperature (871 K).

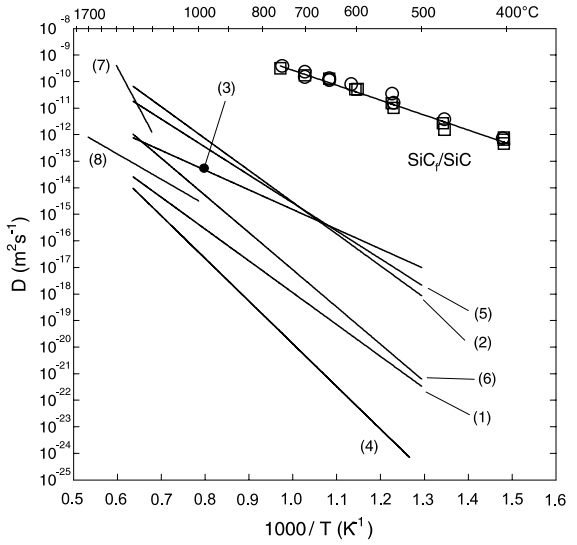

Fig. 4. Comparative Arrhenius plot of the experimental deuterium diffusivities for the composite and the values for hydrogen in different types of monolithic SiC: (1) H_T in α-SiC single-crystal [1], (2) H_T in β-SiC single-crystal [1], (3) H_T in Al doped α-SiC single-crystal [1], (4) H_T in vapour deposited β-SiC [1], (5) H_T in hot pressed α-SiC [1], (6) H_T in sintered β-SiC [1], (7) H_P in KT-SiC [3], (8) $\{1\%H_T, 99\%H_D\}$ in vapour deposited β-SiC [10]. The squared points correspond to the first batch, the circled one to the second.

non-connected porosity or amorphous silicon carbide clusters; the free carbon of the interphase layer covering the fibre preform may be another important cause of deuterium trapping. The departure from Sieverts' law is the motive why here solubility values have been derived instead of Sieverts' constants.

A series of measurements (loading-release) have been performed with deuterium (high purity: 99.7wt%) over the temperature range 675–1029 K and loading pressure 10^5 Pa. A non-linear least-squares fitting routine is run for each measurement with Eq. (1) as the function to reproduce the experimental pressure rise. The effective transport parameters, D and S, are obtained as fitting variables for each group of specimens at each temperature.

The experimental transport parameters, diffusivity and solubility, obtained are depicted in Figs. 3 and 4 together with their respective Arrhenius fittings and the values for monolithic SiC available in the open literature. It is worth mentioning that a negligible difference has been observed between results corresponding to each set of specimens. The different manufacturing procedure in the two types of specimens has not induced any significant change in the transport parameters. Consequently, a unique Arrhenius tendency has been obtained for diffusivity and solubility of both groups:

$$\text{Diffusivity}: D\ (\mathrm{m^2 s^{-1}}) = 1.1\ (\pm 0.7) \times 10^{-4} \exp[-107.7\ (\pm 4.5)\ (\mathrm{kJ/mol})/RT],$$

$$\text{Solubility}: S\ (\mathrm{mol\,m^{-3}}) = 1.9\ (\pm 0.9) \times 10^{3} \exp[-30.2\ (\pm 3.3)\ (\mathrm{kJ/mol})/RT]$$

With respect to the diffusivity (Fig. 4), it can be appreciated that the behaviour of the composite largely departs from the known Arrhenius tendencies of different types of SiC. The diffusivity values are much higher than those reported for SiC, probably because of the accelerated migration through the extensive porosity of the matrix [3]. The activation energy of diffusion reported here (107.7 kJ/mol) is the lowest in comparison with the range of values for SiC, but is still much higher than the reference values for metals and alloys (e.g. E_d was 11.3 kJ/mol for H_D diffusion in OPTIFER-IVb [12]). A comparable diffusion energy ($E_d = 110$ kJ/mol) was reported by Jung [18] for helium in SiC.

Regarding solubility (Fig. 5), it is worth noting that different types of SiC [1,3,10] are exothermic absorbents whereas the composite does not show such behaviour. The reason for this departure may be found in the different nature of the dissolution mechanism, i.e. trapping in internal closed porosity and other micro-structural defects (amorphous SiC-clusters in the matrix) in comparison to the dissolution in interstitial sites of a

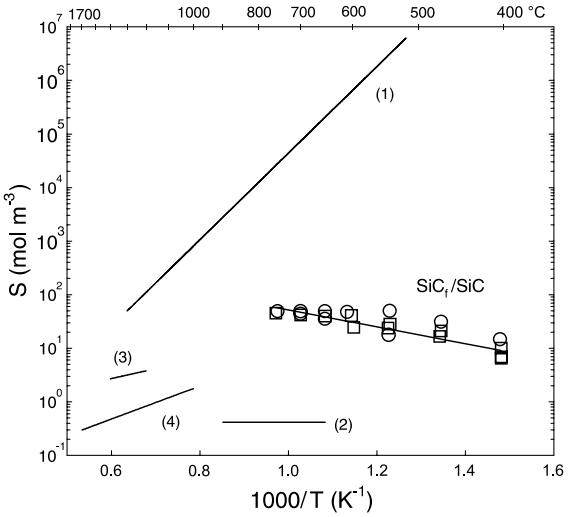

Fig. 5. Comparative Arrhenius plot of the experimental deuterium solubilities ($p = 10^5$ Pa) for the composite and the values for hydrogen in different types of monolithic SiC: (1) H_D in vapour deposited β-SiC [1], (2) H_P in sintered SiC [2], (3) H_P in KT-SiC [3], (4) $\{1\%H_T, 99\%H_D\}$ in vapour deposited β-SiC [10]. The squared points correspond to the first batch, the circled one to the second.

well-ordered SiC lattice. Another possible feature influencing on the solubility disparity is the presence of heterovalent impurities introduced with the matrix precursors for fibre preform densification.

6. Conclusions

The isovolumetric desorption technique has been undertaken in a SiC_f/SiC composite, a suitable low activation structural material for the components of a future thermonuclear reactor. This gas evolution method has been accomplished with H_D over a wide range of temperatures, from 675 to 1029 K, with driving pressures from 1.3×10^4 to 10^5 Pa.

The transport parameters, solubility and diffusivity, have been derived for the composite revealing a considerable departure from the reported values of monolithic SiC. Sieverts' law has not been verified, the main possible phenomena causing this departures are identified.

A negligible variation of deuterium transport parameters has been accounted between the two sets of specimens manufactured using different variants of the hybrid CVI/PIP technique. Consequently, the best manufacturing option may be selected on the basis of the optimisation of the thermo-mechanical properties.

References

[1] R.A. Causey, J.D. Fowler, C. Ravanbakht, T.S. Elleman, K. Verghese, J. Am. Ceram. Soc. 61 (1978) 221.
[2] H. Katsuta and Y. Katano, Hydrogen solubility in silicon carbide and silicon nitride, International Symposium on Fusion Reactor Blanket and Fuel Cycle Technology, 27–29 October 1986, University of Tokyo.
[3] K. Verghese, L.R. Zumwalt, C.P. Feng, T.S. Elleman, J. Nucl. Mater. 85&86 (1979) 1161.
[4] P. Fenici, A.J. Frias Rebelo, R.H. Jones, A. Kohyama, L.L. Snead, J. Nucl. Mater. 258–263 (1998) 215.
[5] A.S. Pérez Ramírez, A. Caso, L. Giancarli, N. Le Bars, G. Chaumat, J.F. Salavy, J. Szczepanski, J. Nucl. Mater 233–237 (1996) 1257.
[6] H. Golfier, G. Aiello, M.A Fütterer, A. Gasse, L. Giancarli, Y. Poitevin, J.F. Salavy, Y. Severi, J. Szczepanski, Proceedings of the ISFNT 5, Roma, Italy, 19–24 September 1999.
[7] S. Ueda, S. Nishio, Y. Seki, R. Kurihara, J. Adachi, S. Yamazaki, J. Nucl. Mater 258–263 (1998) 1589.
[8] S. Sharafat, F. Najmabadi, C.P.C. Wong, Fus. Eng. Des. 18 (1991) 215.
[9] P. Norajitra, L. Bühler, U. Fischer, K. Kleefeldt, S. Malang, G. Reimann, H. Schnauder, L. Giancarli, H. Golfier, Y. Poitevin, J.F. Salavy, Proceedings of the 21st SOFT, Madrid, Spain, 11–15 September 2000.
[10] R.A. Causey, W.R. Wampler, J.R. Retelle, J.L. Kaae, J. Nucl. Mater. 203 (1993) 196.
[11] B. Riccardi in: Development of an advanced CVI-PIP process, FUS TN DEMO, Frascati, 2000. Final report: TASK LONG TERM ADV 1.3.1, 1999 and TTMA-001.7, 2000.
[12] G.A. Esteban, A. Perujo, K. Douglas, L.A. Sedano, J. Nucl. Mater. 281 (2000) 34.
[13] L.A. Sedano, A. Perujo, C.H. Wu, J. Nucl. Mater. 273 (1999) 285.
[14] G.A. Esteban, A. Perujo, L.A. Sedano, K. Douglas, J. Nucl. Mater. 295 (2001) 49.
[15] L.A. Sedano, Obtaining H Interaction Parameters for Carbon Fibre Composites by Modelling Isovolumetric Desorption Experiments, Euroreport: EUR 17320 EN.
[16] L.A. Sedano, S. Alberici, A. Perujo, J. Camposilvan, K. Douglas, J. Nucl. Mater. 258–263 (1998) 662.
[17] G.A. Esteban, A. Perujo, L.A. Sedano, B. Mancinelli, J. Nucl. Mater. 282 (2000) 89.
[18] P. Jung, J. Nucl. Mater. 191–194 (1992) 377.